A highly sensitive quartz-crystal microbalance for sputtering investigations in slow ion–surface collisions

G. Hayderer, M. Schmid, P. Varga, HP. Winter, and F. Aumayr[a)]
Institut für Allgemeine Physik, TU Wien, Wiedner Hauptstrasse 8-10, A-1040 Wien, Austria

(Received 19 April 1999; accepted for publication 27 May 1999)

A quartz-crystal microbalance technique for measuring total sputter yields in ion–surface collisions is described. The electronic circuit to drive the quartz crystal ensures low noise and high frequency stability. By measuring total sputter yields for impact of singly charged ions on LiF target films a sensitivity limit of 0.5% of a monolayer per minute could be achieved. © *1999 American Institute of Physics.* [S0034-6748(99)03509-1]

I. INTRODUCTION

Since it was introduced by Sauerbrey in 1959,[1] the quartz-crystal microbalance (QCM) has been used as a sensitive device for the measurement of small mass changes.[2,3] Presently, it is applied, e.g., for the monitoring of thin film growth in deposition and sputter processes.[4–7] In recent years, a variety of QCM applications in gaseous and liquid environments[8,9] such as gas chromatography detector, gas sensor, biosensor, diagnostic tool for plasma–wall interaction,[10] and solution-phase electrochemistry[11] have been reported.

In order to measure total sputter yields (including both neutral and charged secondary particles) in ion–surface collisions a sensitive quartz-crystal microbalance technique has been developed at TU Wien.[6,7,12,13] In this experiment the target material is first deposited on the quartz crystal as a thin polycrystalline film and then bombarded by slow (<5 keV) singly or multiply charged ions, with the sputter yield being determined from the mass loss of the target film. Whereas quartz crystals are widely used for determination of the area mass and hence the thickness of deposited material, the rate for material removal has mainly been studied with other techniques such as the conventional microbalance, secondary neutral mass spectrometry (SNMS) or catcher foils[14,15] subsequently analyzed by Rutherford backscattering. This is not astonishing because the use of quartz crystals for direct sputter yield measurements encounters severe problems. The rates of material removal and hence the frequency changes are rather low compared to most deposition applications, requiring a rather high frequency stability of the crystal and of the oscillator circuit as well as high accuracy and resolution in determining the resonance frequency. Furthermore, a substantial amount of energy is deposited by the primary particles on the sputtered surface, causing problems due to thermal drift. In many deposition applications, the energy deposition per incident atom is only a few eV (sublimation energy plus heat radiation from the evaporation source), while in the case of sputtering the energy deposited per impinging projectile is rather in the range of a few hundred eV up to several keV. Other problems arise from the sensitivity of the resonance frequency to surface stress induced by, e.g., sputter induced defects, implantation of projectile ions and nonuniformal mass removal across the ion beam impact area.[16–18]

To detect mass changes in the order of 10^{-3} monolayers (ML) per minute, at a typical resonance frequency of 6 MHz the QCM technique requires a frequency stability of a few mHz during this time. This level of performance is today readily achieved with quartz crystals and oscillators designed for timebase applications. Using the quartz crystal as a microbalance in UHV imposes some constraints on the setup, however, such as the necessity of a cable between the quartz crystal and the electronics and the use of an unhoused crystal with one electrode grounded. Under these conditions, customary electronic oscillators cannot provide the required specifications. We have therefore designed new electronics and a special quartz-crystal holder to achieve the requirements for also measuring very low mass changes induced by ion–surface collisions.

II. EXPERIMENTAL METHOD

The mass-sensitive part of the QCM is a planoconvex disk cut from a quartz crystal with resonance frequency in the range of 6 MHz, onto which gold electrodes have been deposited. We have used SC-cut 6 MHz crystals (13.95 mm diameter) with gold electrodes available from KVG Quartz Crystal Technology GmbH, Germany, which are stress compensated (SC). In contrast to the commonly used AT-cut (YXl)-35.25° (nomenclature after IEEE Standard 1978[19]) the SC-cut (YXwl) 21.93°, −33.93° has a resonance frequency insensitive to radial stress and is therefore better suited for our current application.

In the following we describe the experimental procedure for the case of a LiF target film (other targets as Au, Si, GaAs, etc. have been used as well). On one of the metal electrodes a thin polycrystalline LiF film of approximately 200 nm has been deposited in a commercial high vacuum coating system (Leybold L560/HV8.2, 10^{-6} mbar background pressure) with a deposition rate in the order of 10 nm/s. LiF was evaporated from a Mo boat; the substrate

a)Author to whom correspondence should be addressed; electronic mail: aumayr@iap.tuwien.ac.at

 © 1999 American Institute of Physics

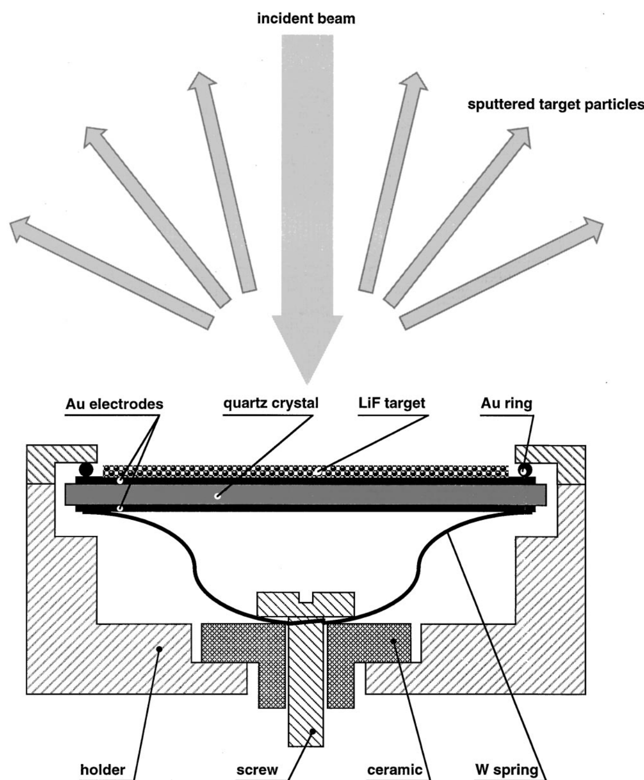

FIG. 1. Experimental setup (schematically).

temperature was kept at approximately 150 °C during deposition. The quartz crystal with the target film was transported in air to the UHV facility, where it was attached to the target holder. To minimize stress in the quartz crystal from its mounting, we used a thin Au ring on the LiF surface and fixed the quartz crystal on the other side with a W spring (Fig. 1). The Au ring and the W spring also served as electrical contacts for the connection between the electronic circuit and the quartz crystal.

To minimize the effect of thermal drifts and fluctuations, the quartz crystal is operated at the minimum of its resonance frequency versus temperature curve (Fig. 2). From a careful temperature scan this minimum was determined to be 191 °C (Fig. 2), which means that the LiF target film is also being kept at this temperature during sputtering measurements.

Since the deposited target film is very thin compared to

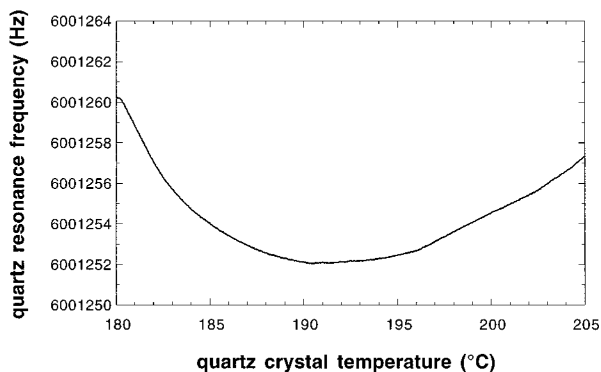

FIG. 2. Resonance frequency of the quartz crystal measured vs quartz temperature.

the thickness of the quartz crystal, it is sufficient to use the simple equation according to Sauerbrey:[1]

$$\frac{\Delta m}{m} = -\frac{\Delta f}{f}, \tag{1}$$

which relates the relative mass loss $\Delta m/m$ to the relative change of the resonance frequency $\Delta f/f$. For a quartz crystal with resonance frequency f, mass density ρ_{quartz}, and thickness l_{quartz} the mass removal of sputtered particles Δm per unit area (in atomic mass units per square centimeter) is given by

$$\Delta m(\text{amu/cm}^2) = -\frac{\rho_{\text{quartz}} l_{\text{quartz}}}{f(\text{Hz}) m_n} \times \Delta f(\text{Hz}), \tag{2}$$

with $m_n = 1.66 \times 10^{-27}$ kg. To determine the total sputter yield one also has to measure the time integrated incident ion current per unit area:

$$\int I(t) dt/A. \tag{3}$$

Then the average mass removal y per incident projectile in charge state q can be calculated from ($e_0 \ldots$ electron charge)

$$y[\text{amu/ion}] = \frac{(\rho_{\text{quartz}} l_{\text{quartz}})/(f m_n)}{[\int I(t) dt]/(e_0 q A)} \times \Delta f(\text{Hz}). \tag{4}$$

This average mass removal per incident projectile y is related to the total sputter yield Y by

$$Y = \frac{y}{m_t}, \tag{5}$$

with m_t being the target particle mass. A biased Faraday cup with pinhole area A has been used for measuring the primary ion current density.

Our technique does not suffer from problems inherent to collection of sputtered particles as incompletely defined collection geometry and/or unknown neutral particle sticking coefficients, since the total sputter yields can be readily determined from the frequency change for known ion current density.

There is, however, a non-negligible effect of mass change due to primary ion implantation. At low ion dose this causes a frequency change in the opposite sense as sputtering. Steady state conditions can however be reached at higher ion doses, when the amount of sputtered implanted atoms equals the amount of freshly implanted projectile ions. For each projectile-target combination the necessary dose to reach steady state conditions depends on the projectile energy and has to be determined experimentally by measuring y as a function of ion dose. For example, for 100 eV Ne^+ impact on LiF, after a total dose of 1×10^{16} ions/cm^2, which corresponds to the removal of two monolayers, the measured sputtering rate did not change significantly any more (within our accuracy of $\pm 5\%$). Of course one could argue that the quantity measured in this way is not the sputter yield of a ''virgin'' surface. It is, however, the quantity of interest for ''real life'' sputtering applications, where sputtering always proceeds under fairly high ion doses.

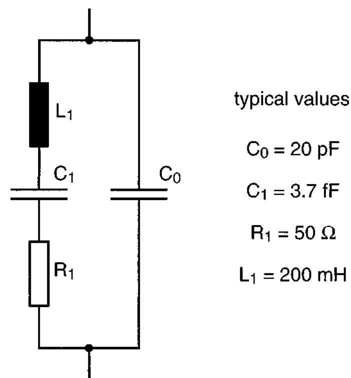

FIG. 3. Butterworth–van Dyke equivalent circuit of a quartz crystal. Typical values of the 6 MHz SC-cut crystal are given.

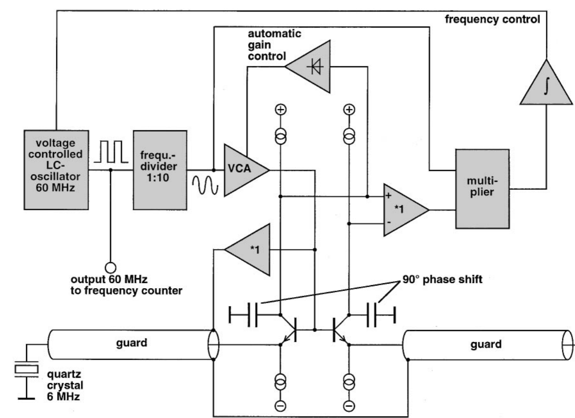

FIG. 4. Block diagram of the electronics driving the quartz crystal at its resonance frequency.

A further problem has to be taken care of, which arises from the nonuniformal mass removal due to an inhomogeneous ion beam cross section. In such cases significant deviations from the Sauerbrey Eq. (1) have to be expected because of the appearance of dominant overtone frequencies.[16] In our experiment we achieve uniformal sputtering by scanning the ion beam by means of deflection plates across the entire active area of the quartz crystal (typical frequency of 1.4 kHz).

III. ELECTRONICS

In the following we will describe our electronics which has been specifically designed to assure high sensitivity and stability. The primary tasks of this circuit are to drive the quartz crystal in series resonance at its fundamental oscillation of about 6 MHz and to measure this resonance frequency precisely within a few mHz. The frequency of the series-resonance f_s is determined by the elements L_1, C_1, and R_1 in the Butterworth–van Dyke equivalent circuit of the crystal (Fig. 3), and it is the natural frequency of the crystal with its electrodes shorted. In contrast to the parallel resonance frequency (open electrode), f_s can be determined if the crystal is connected to the electronics via a cable with additional capacitance parallel to C_0. Oscillator circuits for series resonance amplify a signal proportional to the current through the quartz crystal and backfeed this voltage. This selects the resonance with the highest admittance. In contrast to AT cut crystals, the SC cut crystals have two shear modes driven by the piezoelectric effect, with the temperature and stress compensated C mode having a lower piezoelectric coupling factor ($k^2=0.024$) than the unwanted B mode ($k^2=0.026$). Therefore, the B mode, which has a resonance frequency approximately 10% above that of the C mode, usually has a higher admittance and must be suppressed. In oscillator circuits, this can be done via a LC filter, which causes, however, disadvantageous phase shift giving rise to additional frequency drift. This problem can be solved by using a separate oscillator which locks on the crystal's resonance frequency, similar to a phase locked loop (PLL). The phase difference between the driving voltage at the crystal and the current passing through is used to control the oscillator's frequency.

The circuit is shown schematically in Fig. 4 (the detailed electronic schematics are available from the authors upon request). We use a low noise LC oscillator (Clapp type) tunable between 59 and 61 MHz by varicaps. After amplification and conversion to TTL levels, the oscillator signal is fed on the one hand into the frequency counter and on the other hand into a Johnson counter dividing the frequency by 10 for driving the quartz crystal. This setup uses the same digital signal for the analog part of the circuit and the frequency counter, thereby minimizing jitter and drift of the trigger setpoint which would affect the frequency measurement when connecting the frequency counter to the analog electronics. After smoothing to sinusoidal shape, the 6 MHz signal passes through a voltage controlled amplifier (VCA)

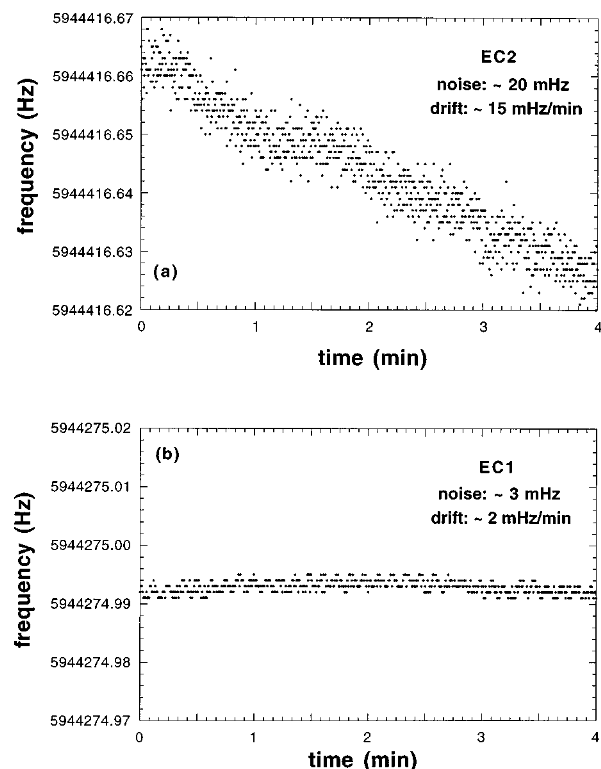

FIG. 5. Comparison of measured frequency drift and noise for previously used (a) electronics EC2 and the newly designed (b) electronics EC1 (cf. Fig. 3), respectively.

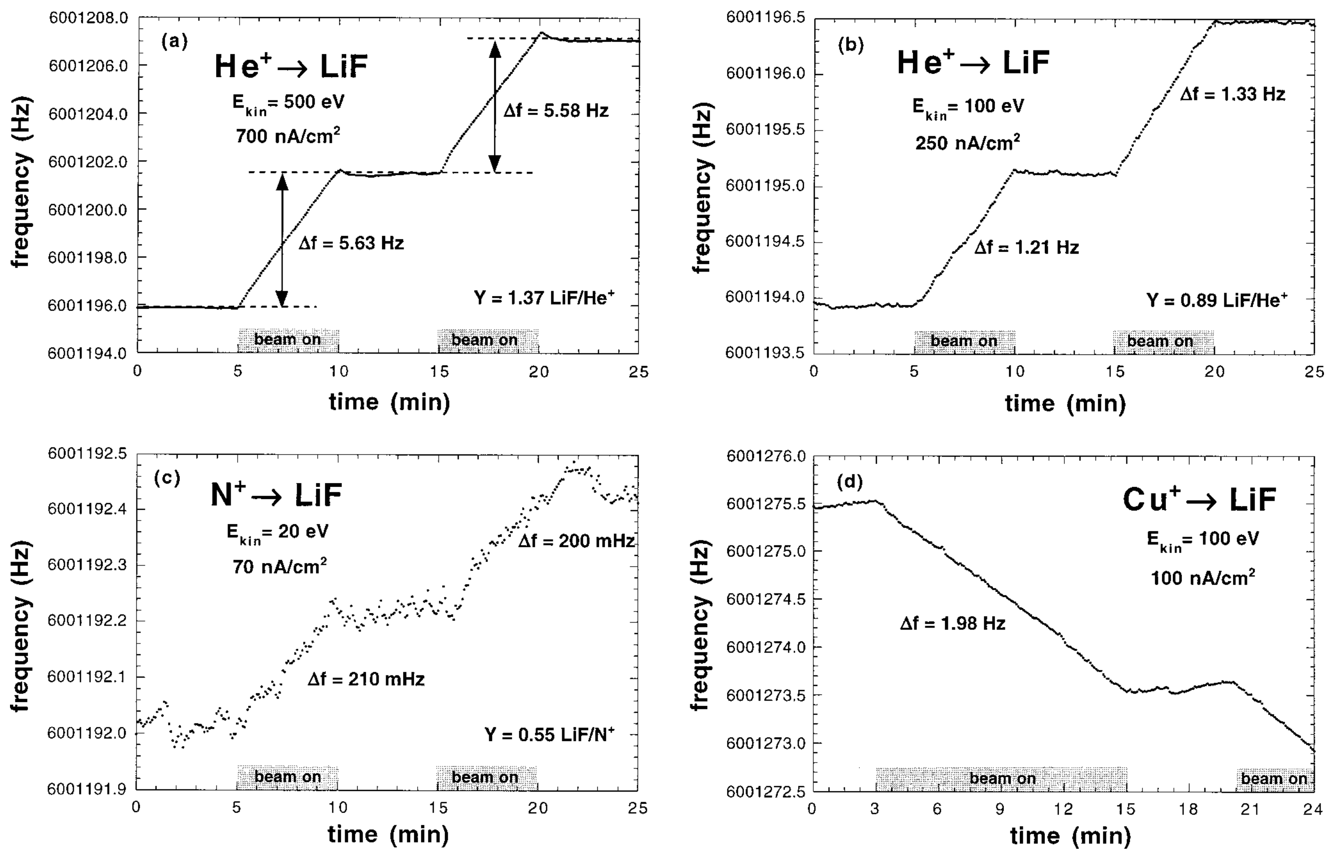

FIG. 6. Typical raw data obtained in sputtering measurements of LiF by various singly charged ions (a)–(d) with the QCM technique.

which keeps the current through the crystal and hence its vibration amplitude constant.

Since it is not feasible to place the electronics inside the UHV chamber (need for baking up to 250 °C), we have to apply electrical feedthroughs and 50 cm connection cables with an additional parallel capacity to the quartz-crystal capacity C_0. We therefore use an active compensation of this parallel capacity consisting of two branches, which are identical except at the end where only one branch is connected to the quartz crystal. Both branches are assured to have the same additional parallel capacity, so that the signal from the compensation branch can be used to correct the signal in a differential amplifier. The cables are tightly packed and the shielding of the coaxial cables are connected as guard leads, which further minimizes the phase shift.

The current through both branches is converted to 90° shifted voltages by two capacitors. Their difference, which is proportional to the 90° phase shifted current through the quartz crystal, finally reaches a multiplier for phase comparison with the voltage at the crystal. At series resonance, voltage and current of the crystal are in phase, leading to a 90° phase shift at the multiplier's input. Any deviation from the crystal's resonance frequency f_s results in a phase shift and thus nonzero multiplier output. This error signal increases or decreases the oscillator frequency and thereby keeps the oscillator frequency at exactly 10 f_s.

As the required stability of the phase shift is very high ($\sim 10^{-4}$ rad), sufficiently fast electronic components with low phase shift and hence high transit frequencies in the range of 500 MHz must be used. Much attention has to be paid on the circuit layout to avoid undesirable self oscillations of the circuit with frequencies in the range of some hundred MHz.

IV. TYPICAL RESULTS

In a first test the relevance of the above described new electronics (EC1) for frequency stability and noise was investigated and compared to data obtained with the electronics (EC2) used in previous experiments.[12,13] This electronics EC2 was a conventional series resonance oscillator with compensation of parallel capacities. Typical results of this comparison are shown in Fig. 5. Data shown have been measured without ion bombardment to obtain the frequency behavior exclusively due to the electronic circuit and the quartz-crystal holder. The quartz crystal temperature was kept at the minimum of the frequency versus temperature curve (Fig. 2) at 191 °C and the background pressure was kept below 10^{-9} mbar. Use of EC1 reduced noise as well as drift by at least a factor of 5 as compared to EC2.

Some typical raw data of total sputter yield measurements for ion bombardment of a LiF surface are shown in Figs. 6(a)–6(d). ''Beam-off'' periods, where the frequency drift is checked, alternate with ''beam-on'' periods where a frequency change due to sputtering (or deposition) is measured. Figure 6(a) shows data for 500 eV He^+ impact on LiF. The relatively high sputter yield (1.4 LiF molecules per He^+ ion) due to both potential and kinetic sputtering[12] and the fairly high ion current density (700 nA/cm^2) result in a large frequency change ($\Delta f = 5.6$Hz) during the beam-on pe-

riods, which can be conveniently measured. At impact energies around the threshold for kinetic sputtering [100 eV He^+, Fig. 6(b)] not only the total sputter yield but also the ion current density (due to deceleration) are smaller, but the frequency change can still be evaluated with reasonable accuracy [Fig. 6(b)]. Figure 6(c) shows the extremely difficult case of 20 eV N^+ bombardment on the LiF surface. At such a low impact energy no kinetic sputtering takes place. The potential energy stored in N^+ (14.53 eV) is much smaller than for He^+ (24.59 eV), also leading to a correspondingly small potential sputter yield. Due to the strong deceleration when reaching 20 eV impact energy the incident ion current density is only 70 nA/cm^2. The resulting frequency change of only 200 mHz is therefore subject to relatively large errors. From a series of similar measurements with low ion current and small sputter yield we conclude that our method is presently limited to cases where the product of the total sputter yield times the ion current density typically exceeds 0.2 amu/ion μA/cm^2 [for comparison, Fig. 6(c) corresponds to a product of about 1 amu/ion μA/cm^2]. Our QCM is therefore able to detect a removal of as low as 5×10^{10} LiF molecules per cm^2 and second. This results in a sensitivity to mass changes as small as approximately 8×10^{-5} monolayers per second or 0.5% of a monolayer per minute and therefore in an improvement in sensitivity over previously used setups by at least a factor of 5.

Finally, Fig. 6(d) shows the interesting case of 100 eV Cu^+ impact on LiF. Since the recombination energy of Cu^+ (7.73 eV) is too small to cause potential sputtering and the kinetic sputtering yield is also practically zero (threshold region), we observe a net deposition of Cu due to implantation (or sticking) of Cu^+ projectile ions into (onto) the LiF target surface. Suppose the sputter yield of LiF with slow Cu^+ projectiles is zero, implantation of a dose of 4×10^{13} Cu atoms per cm^2 [which corresponds to the Cu^+ ion dose for 1 min for Fig. 6(d)] will lead to a frequency change of 300 mHz per minute, compared to a measured frequency change of 165 mHz/min in Fig. 6(d). Therefore about 55% of the incoming Cu^+ projectiles are implanted or adsorbed on the LiF surface.

ACKNOWLEDGMENTS

This work was supported by Austrian Fonds zur Förderung der Wissenschaftlichen Forschung (Project No. P 12388 PHY) and carried out within Association EURATOM-ÖAW.

[1] G. Sauerbrey, Z. Phys. **155**, 206 (1959).
[2] J. W. Coburn, in *Application of Piezoelectric Quartz Crystal Microbalances,* edited by C. Lu and A. W. Czanderna (Elsevier, Amsterdam, 1984), p. 221.
[3] J. W. Coburn and H. F. Winter, J. Appl. Phys. **50**, 3189 (1979).
[4] C. McKeown, Rev. Sci. Instrum. **32**, 133 (1961).
[5] O. Ellegaard, J. Schou, H. Sorensen, and P. Borgesen, Surf. Sci. **167**, 474 (1986).
[6] T. Neidhart, F. Pichler, F. Aumayr, HP. Winter, M. Schmid, and P. Varga, Phys. Rev. Lett. **74**, 5280 (1995).
[7] E. Benes, M. Gröschl, and F. Seifert, IEEE Trans. Ultrason. Ferroelectr. Freq. Control **45**, 1314 (1998).
[8] O. S. Milanko, S. A. Milinkovic, and L. V. Rajakovic, Anal. Chim. Acta **264**, 43 (1992).
[9] Y. Jane and J. Shih, Analyst **120**, 517 (1995).
[10] D. Bourgoin, G. G. Ross, S. Savoie, Y. Drolet, and E. Haddad, J. Nucl. Mater. **241–243**, 765 (1997).
[11] G. C. Komplin, F. Schleifer, and W. J. Pietro, Rev. Sci. Instrum. **64**, 1530 (1993).
[12] M. Sporn, G. Libiseller, T. Neidhart, M. Schmid, F. Aumayr, HP. Winter, P. Varga, M. Grether, and N. Stolterfoht, Phys. Rev. Lett. **79**, 945 (1997).
[13] T. Neidhart, Z. Toth, M. Hochhold, M. Schmid, and P. Varga, Nucl. Instrum. Methods Phys. Res. B **90**, 496 (1994).
[14] S. T. deZwart, T. Fried, D. O. Boerma, R. Hoekstra, A. G. Drentje, and A. L. Boers, Surf. Sci. **177**, L939 (1986).
[15] T. Schenkel, A. V. Barnes, A. V. Hamza, D. H. Schneider, J. C. Banks, and B. L. Doyle, Phys. Rev. Lett. **80**, 4325 (1998).
[16] J. R. Vig, IEEE Trans. Ultrason. Ferroelectr. Freq. Control **45**, 1123 (1998).
[17] S. Hertl, L. Wimmer, and E. Benes, J. Acoust. Soc. Am. **78**, 1337 (1985).
[18] E. Benes, M. Schmid, and V. Kravchenko, J. Acoust. Soc. Am. **90**, 700 (1991).
[19] *IEEE Standard on Piezoelectricity* (Institute of Electrical and Electronics Engineers, New York, 1978), Vol. 176.